

Fig. S1. Subtyping of GC cell lines to CIMP clusters. Unsupervised hierarchical clustering of 62 GC cell lines based on the top 10,000 most variable CGI probes identified 4 major branches, that was categorized into 3 distinct clusters, designated as ‘CIMP-high’ (branch 1), ‘CIMP-low’ (branches 3, 4) and ‘non-CIMP’ (branch 2). EBV, MSI and mutational status of select cancer genes in each cluster are also indicated. Colour key represents methylation β -values.

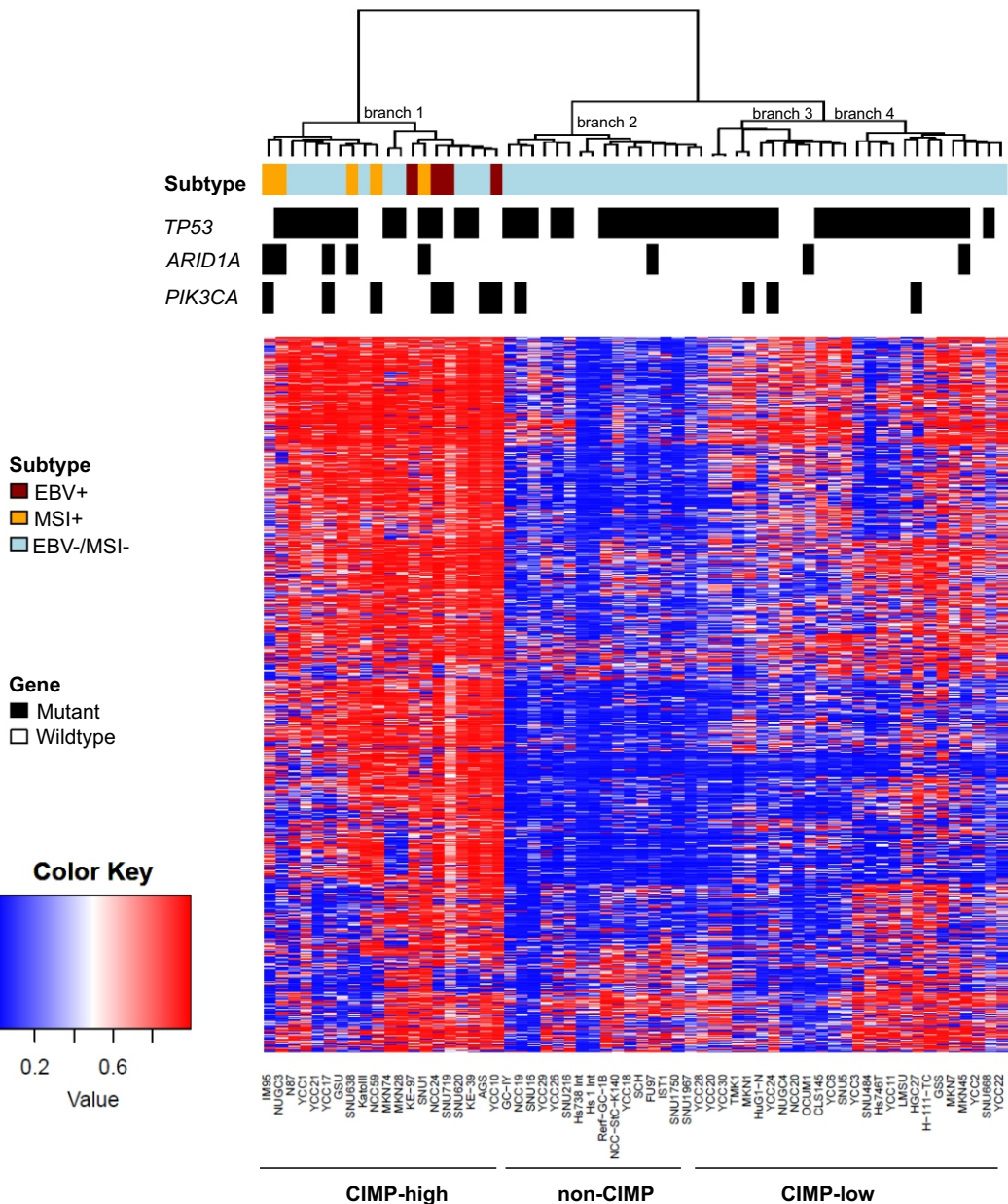
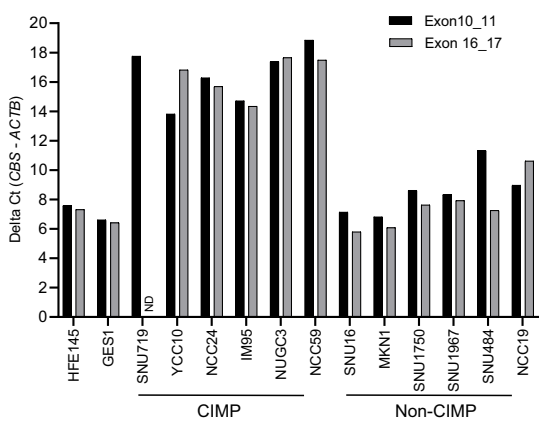


Fig. S2. Validation of CBS RNA and protein levels. **(A)** CBS mRNA expression in normal gastric cell lines [n=2] (Average Delta Ct = 6.8 - 7.0), CIMP lines [n=6] (Average Delta Ct = 16.4), and non-CIMP lines [n=6] (Average Delta Ct = 7.5 - 8.5) assayed by quantitative PCR **(B)** Protein levels of CBS in SNU1750 cell line treated with non-targeting or *CBS* targeted siRNAs [top panel] with knockdown efficiency validated using quantitative PCR [bottom panel] (n=3) (*P<0.05) **(C)** CBS mRNA expression in 24 normal human stomachs assayed by quantitative PCR (Average Delta Ct = 7.6) **(D)** Immunohistochemistry of CBS antibody in human tissue with high CBS mRNA expression, liver [top panel] and low CBS mRNA expression, thigh muscle [bottom panel] according to GTEx portal [Mean TPM of 135.9 in liver and 0.8 in skeletal muscle]. Control sections were not treated with the primary antibody. TPM, Transcripts Per Million; kDa, kilodalton; ND, Not determined.

A**B**

SNU1750 (non-CIMP)

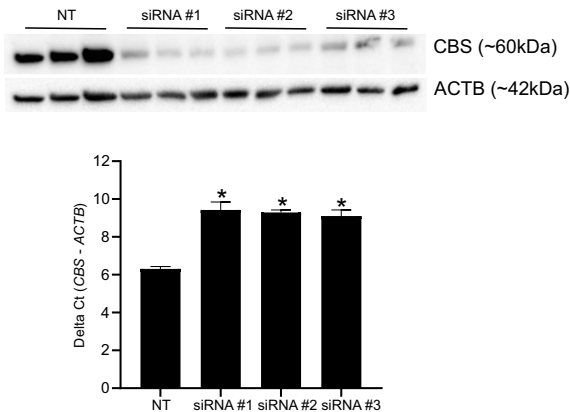
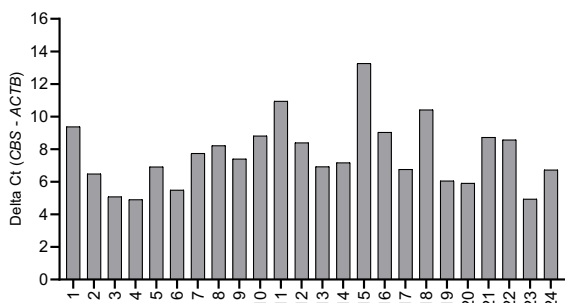
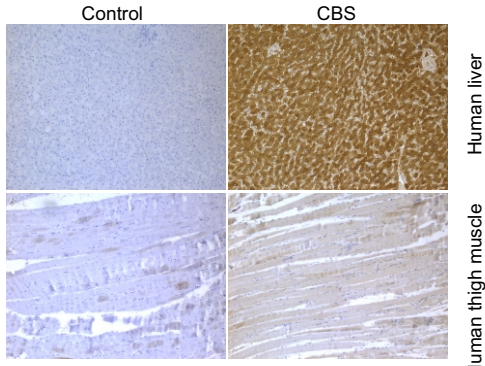
**C****D**

Fig. S3. Uncropped western blotting images. CBS protein levels in **(A)** Normal gastric, CIMP, and non-CIMP GC lines as shown in Figure 1D **(B)** SNU1750 cell line treated with non-targeting or *CBS* targeted siRNAs as shown in Supplementary Figure 2B **(C)** GES1 CRISPR control and *CBS*-deficient CRISPR clones as shown in Figure 4B **(D)** HFE145 CRISPR control, *CBS*-deficient CRISPR clone 1 and clone 2 cells as shown in Figure S9A.

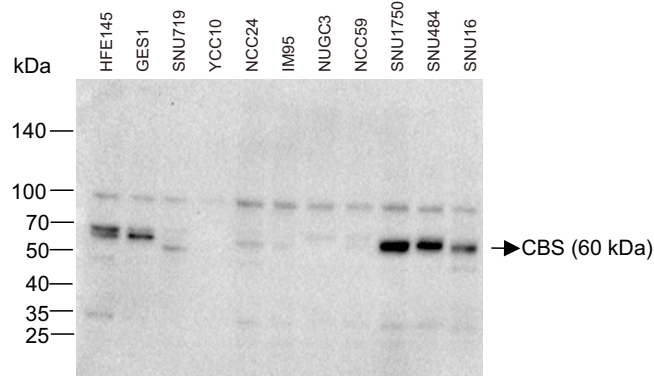
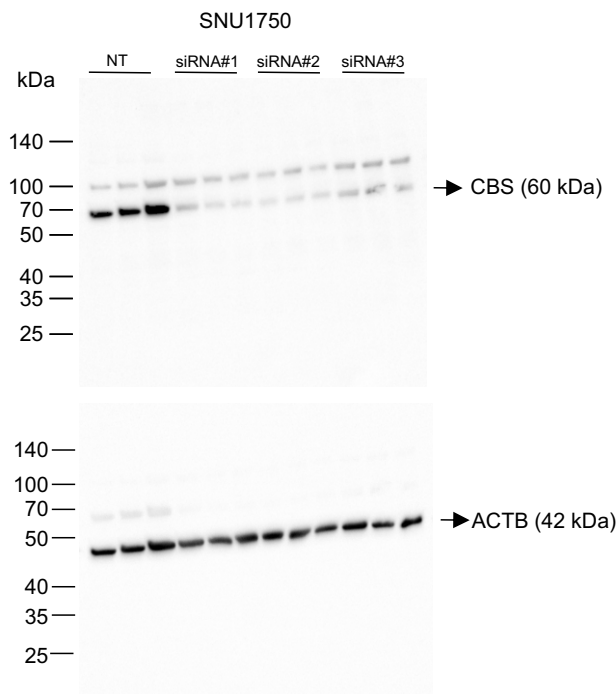
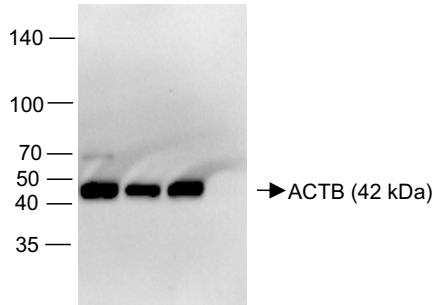
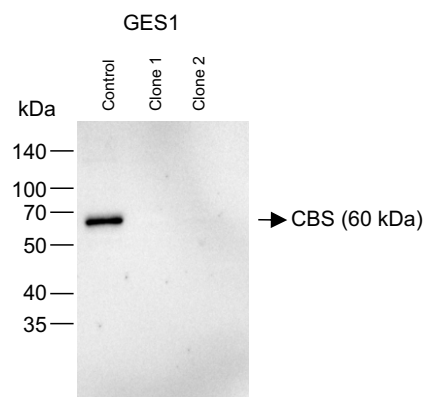
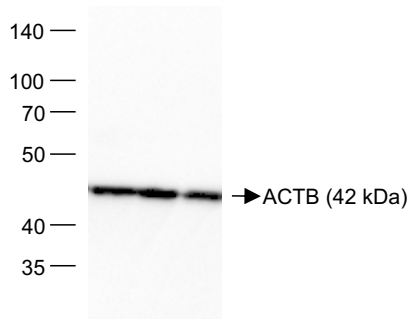
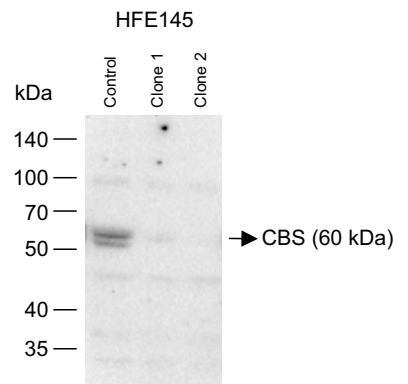
A**B****C****D**

Fig. S4. Lack of H3K27me3 enrichment at *CBS* promoter in GC CIMP cell lines. (A)

Representative example showing enrichment of 5-methyl cytosine [5-mc] at *CBS* promoter in CIMP cell line IM95 (upper panel), and lack of enrichment of H3K27me3 in CIMP cell lines IM95 and AGS (lower panel) in the same region. SNU484 and YCC11 are non-CIMP cell lines. Y-axis for 5-mc tracks represents enrichment over input. Y-axis for H3K27me3 tracks represents reads per kilobase million. **(B)** Positive controls for H3K27me3-ChIP showing enrichment at *ZRANB2-AS1* in AGS, IM95, SNU484 and YCC11 cell lines (left panel) and *LHFPL4* (right panel) in AGS, IM95, and YCC11 cell lines.

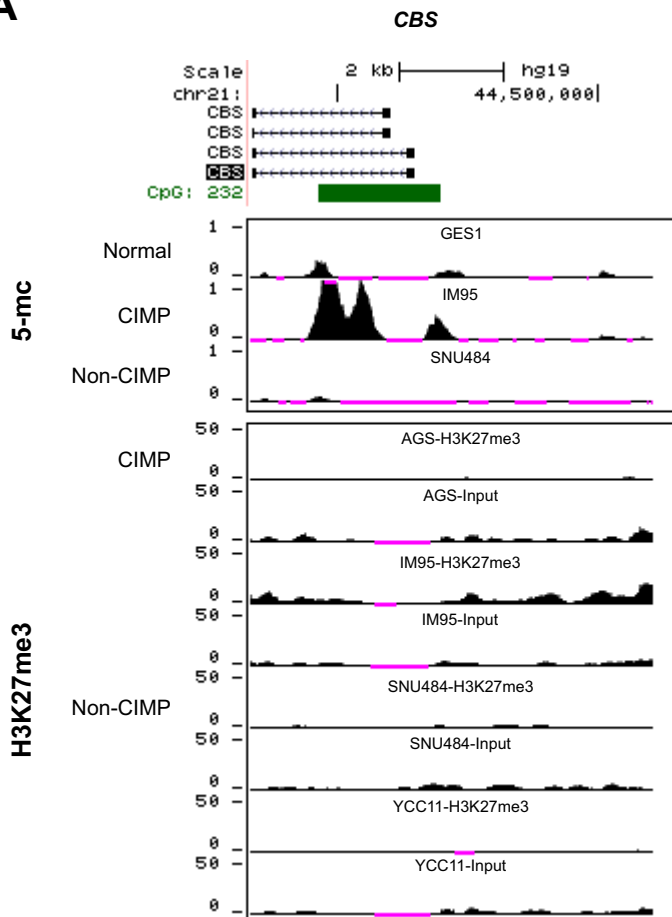
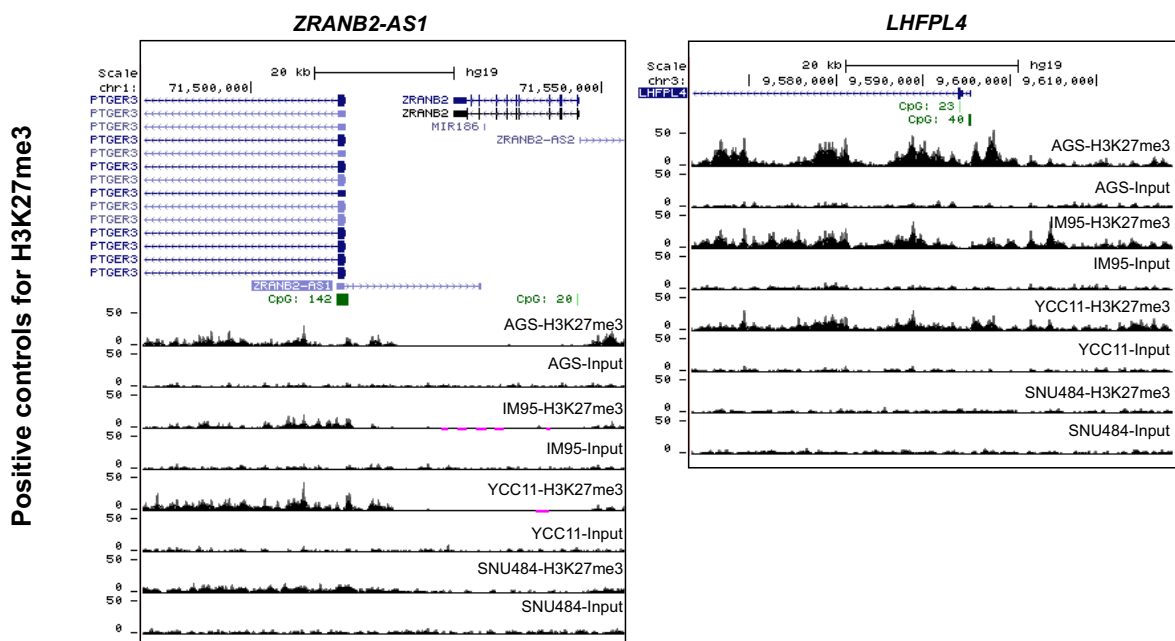
A**B**

Fig. S5. Distribution of *CBS* promoter methylation values in CIMP and non-CIMP categories in multiple tumours. Graph representing the percentage of CIMP and non-CIMP samples in each tumour type harbouring different levels of *CBS* promoter methylation levels based on β -values. CIMP tumours tend to carry higher *CBS* promoter β -values vs. non-CIMP tumours (BLCA: 63.8% vs. 17.1%, UCEC: 29.3% vs. 1.80%, EAC: 93.0% vs. 37.90%, HNSC: 76.7% vs. 17.7%, LIHC: 28.8% vs. 15.6%, STAD: 98.8% vs. 49.2%).

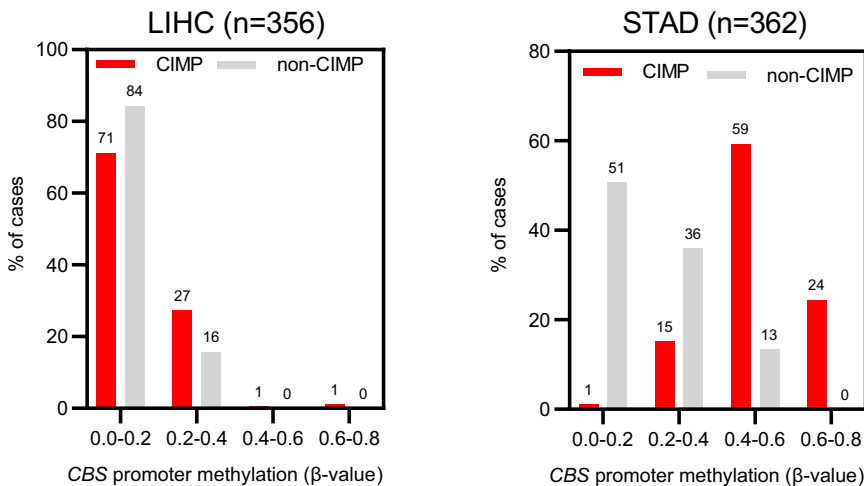
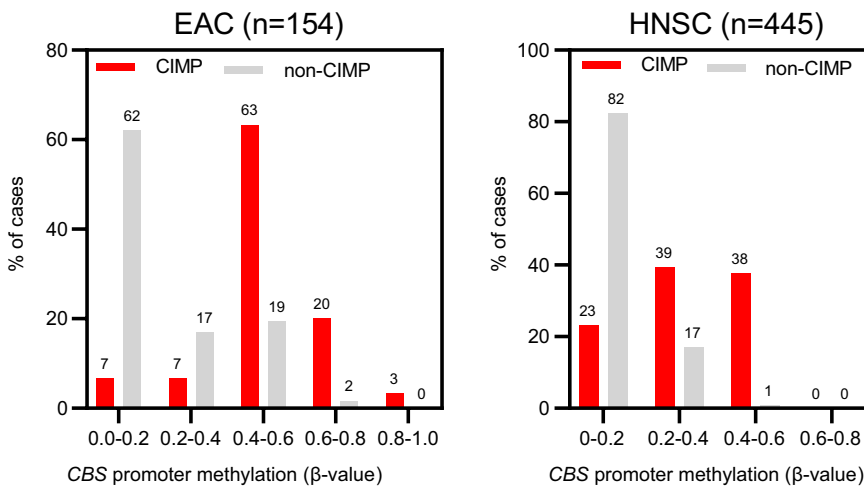
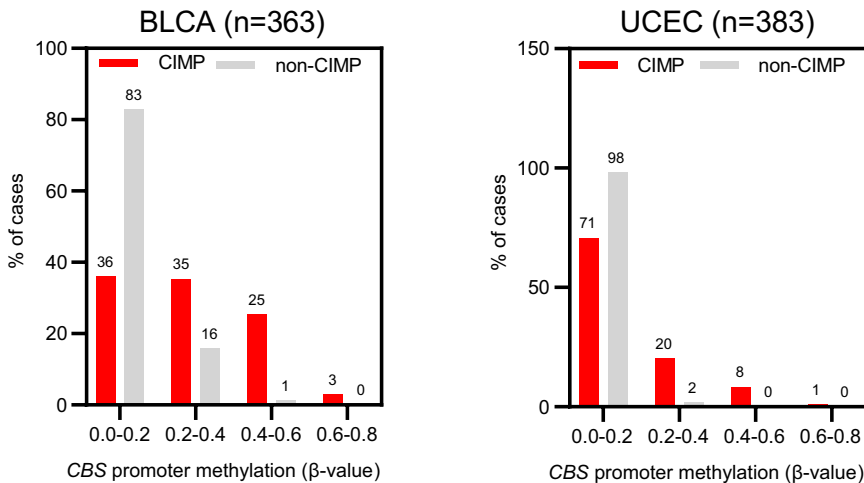


Fig. S6. Correlation plots of *CBS* gene expression and promoter methylation in multiple cancers. Correlation plots of *CBS* gene expression (RSEM) and DNA methylation (β -values) in BLCA, EAC, HNSC, LIHC, UCEC and STAD. Spearman r and P-values are indicated per cancer type.

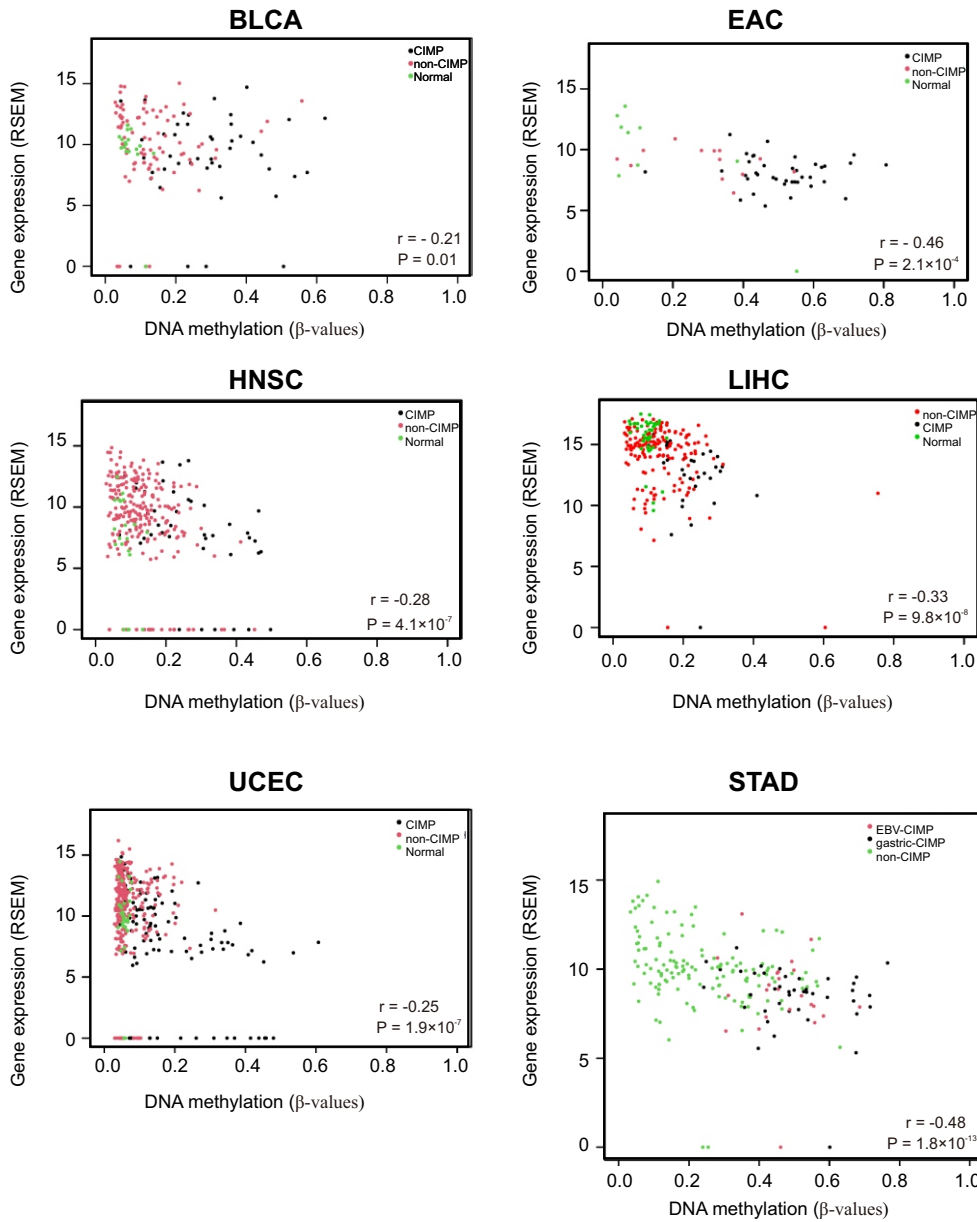


Fig. S7. *CBS* promoter is hypermethylated in Barret's oesophagus. Heat map representing mean methylation β -values of 14 CpG probes in the 5'UTR and TSS region of *CBS* gene in normal, GERD [gastroesophageal reflux disease], NSE [non-tumour squamous oesophagus], BE [Barret's oesophagus], and EAC [Oesophageal adenocarcinoma] groups reported as significant ($P<0.05$) by Krause et al [18].

CBS promoter methylation in Barret's oesophagus

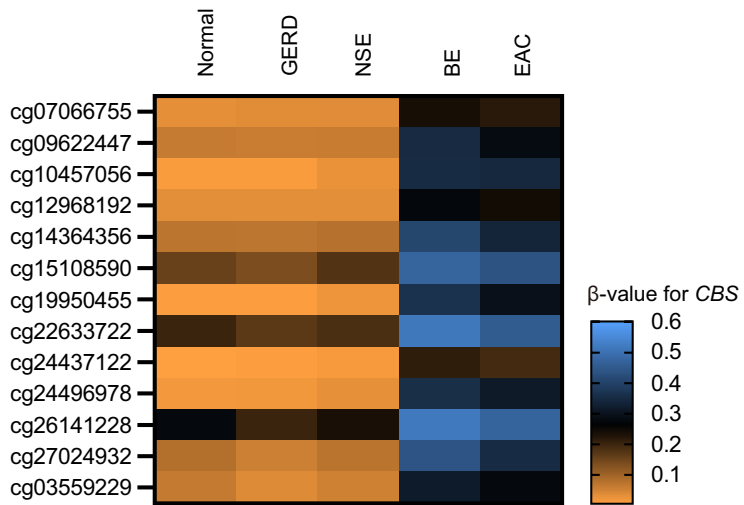


Fig. S8. Venn diagram of differentially methylated probes in random pairing of GES1, parental, CRISPR control and *CBS*-deficient cells. Differential methylation analysis of random pairing of samples (β -value difference ≥ 0.2) across passages indicated no conserved signature.

(Clone 2 and Parental)
vs.
(Clone 1 and CRISPR control)

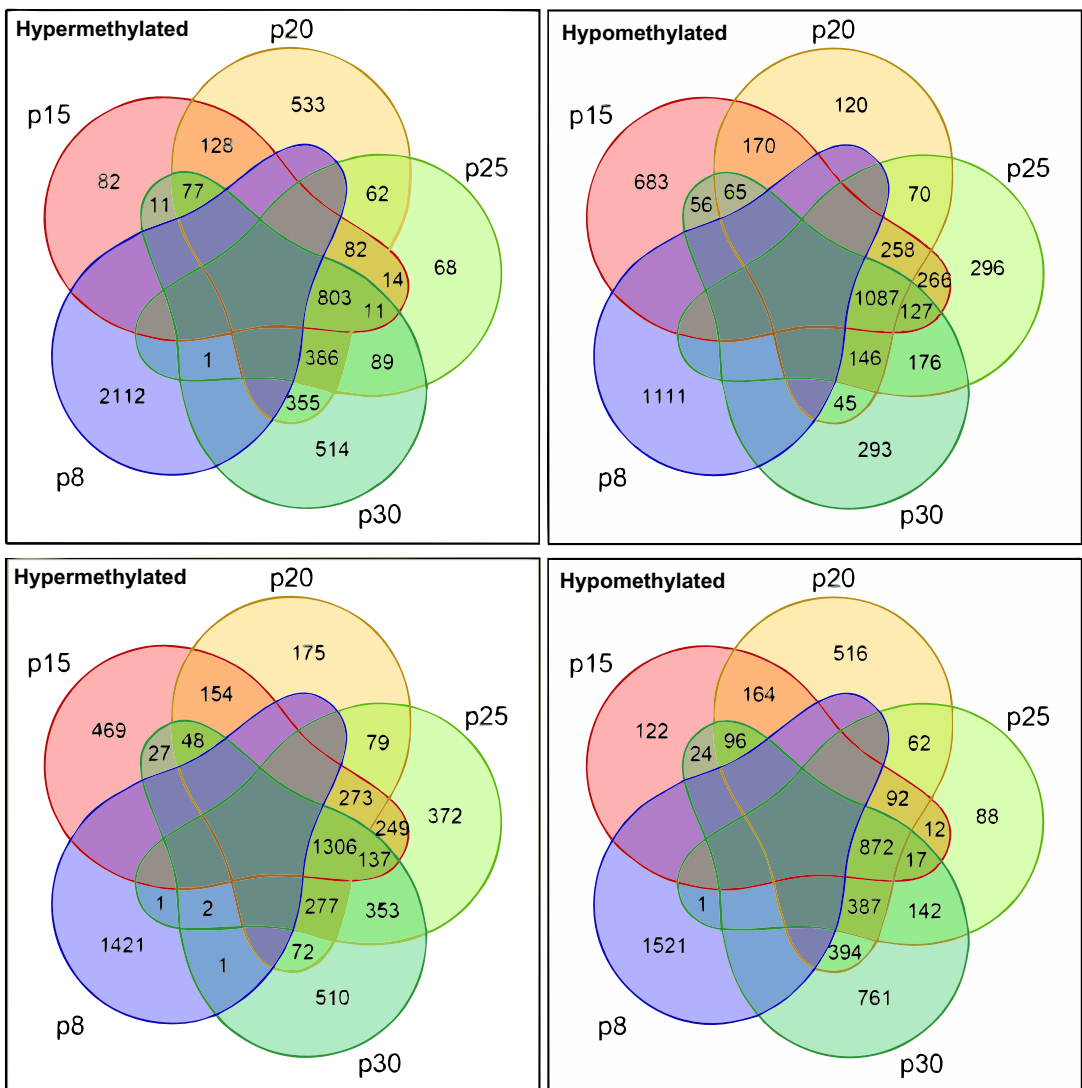
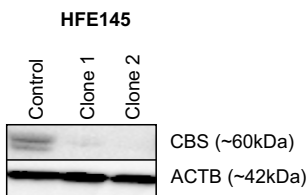


Fig. S9. Loss of CBS alters the DNA methylation landscape in normal gastric epithelial cell line HFE145. (A) CBS protein levels in HFE145 CRISPR control, *CBS*-deficient CRISPR clone 1 and clone 2 cells using Western blotting (B) Venn diagram of differential methylation analysis of HFE145 *CBS*-deficient clone 1 and clone 2 compared to parental and CRISPR control cells (β -value difference ≥ 0.2) between P5 and P23 (C) Venn diagram of differential methylation analysis of random pairing of samples (β -value difference ≥ 0.2) across 2 passages indicated minimal conserved signature (D) Breakdown of the HFE145 *CBS*-deficient conserved signature in CpG contexts island, shore, shelf and open sea; * p<0.001 according to binomial test; ‘Annotated’ refers to the distribution of CpG probes on the Infinium methylation EPIC array, ‘Random’ refers to the sum of all differentially methylated CpG probes in random pairing of samples (E) Unsupervised clustering of conserved hypermethylated 3241 CpG sites in HFE145 *CBS*-deficient clones separates them from parental and CRISPR control cells (F) Enrichment of PRC2-related factors in *CBS*-deficient conserved hypermethylation signatures. kDa, kilodalton.

A**B**

(Clone 1 and Clone 2) vs. (Parental and CRISPR control)

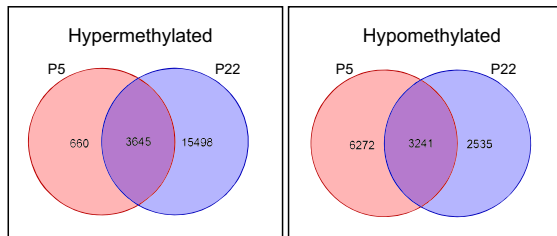
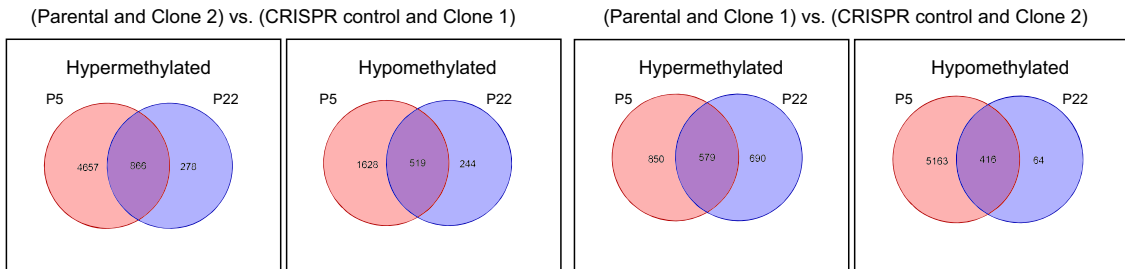
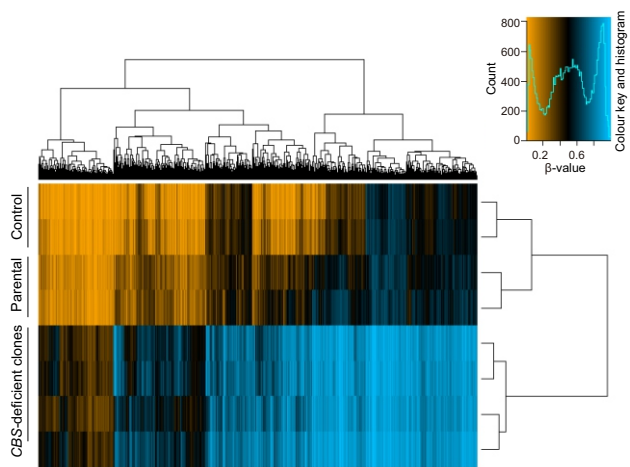
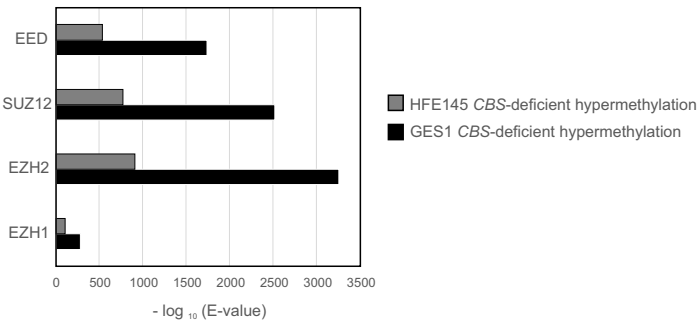
**C****E****F**

Fig. S10. CBS-deficiency causes altered metabolic state in normal gastric cells with significant dysregulation of lipids. (A) Pie charts representing metabolic changes in *CBS*-deficient GES1 and HFE145 cells (upper panel) and list of conserved metabolites (lower panel) (B) Gene expression levels (FPKM) of *NNMT* in *CBS*-deficient clones compared to controls (C) Heat map of significantly altered lipids ($P < 0.05$) in *CBS*-deficient clones compared to controls; red underline indicates conserved metabolites between cell lines.

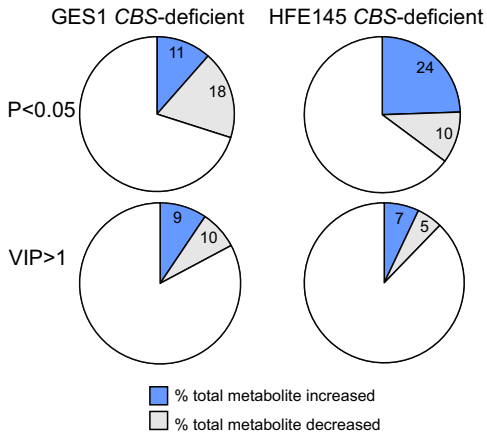
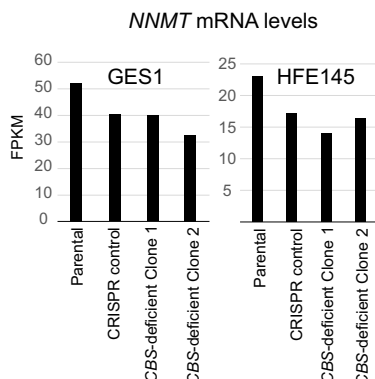
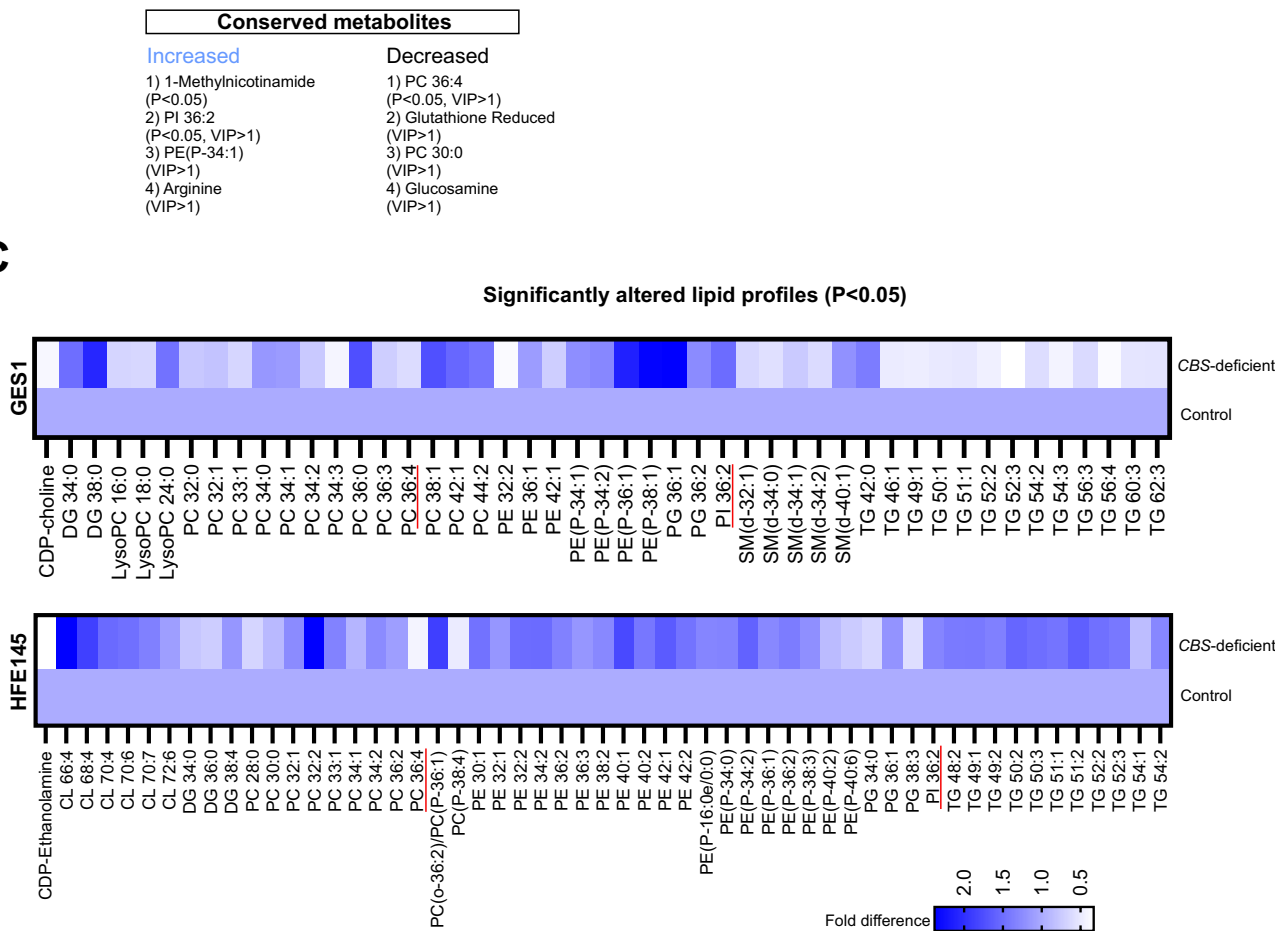
A**B****C**

Fig. S11. Proposed model for *CBS* epimutation in GC. Epimutation at the promoter locus of *CBS* remodels normal gastric epithelial cells through simultaneous perturbation of the methionine and homocysteine cycles. This results in reshaping of the DNA methylation landscape, and an intrinsic inflammatory cellular response. Pre-malignant gastric intestinal metaplasia lesions with *CBS* hypermethylation may thus be more prone to chronic inflammation and benefit from anti-inflammatory H₂S donor therapies. *CBS* loss influences DNA methylation likely through multiple mechanisms. CIMP, CpG island methylator phenotype; EBV, Epstein - Barr virus; MSI, Microsatellite instability.

